An Extension of MAT_240 to Consider the Failure of Structural Adhesive Joints in Crash Simulations

Stephan Marzi[1]
[1]Fraunhofer IFAM, Bremen, Germany

Summary:

MAT_COHESIVE_MIXED_MODE_ELASTOPLASTIC_RATE, or in short MAT_240, is a cohesive zone model, which has been recently developed to consider the failure behaviour of structural joints in crash simulations. The model is applicable to different kinds of structural joints as adhesively bonded or spot/seam welded joints, but its development focused on the efficient crash simulation of structural adhesive joints of small layer thickness. However, tolerances in the manufacturing process may lead to a larger adhesive layer thickness.

In the present work, MAT_240 has been extended via a user-defined subroutine to consider the dependency of the critical energy release rates G_{Ic} and G_{IIc}, which are model parameters of MAT_240, on the thickness of an adhesive layer. While the fracture energy G_{Ic} under Mode I loading is evaluated in Tapered Double Cantilever Beam (TDCB) tests, the End-Loaded Shear Joint (ELSJ) test is used to analyze the Mode II fracture behaviour. Five adhesive layer thicknesses, ranging from 0.25 to $4.0\,\mathrm{mm}$, were investigated for both fracture modes. All tests have been performed at quasi-static test conditions.

The experimentally detected correlations between the critical energy release rates and the adhesive layer thickness are implemented into the user-defined cohesive zone model, which is based on MAT_240. Simulations of asymmetric tapered double cantilever beam (ATDCB) tests, which exhibit an adhesive layer loaded in mixed-mode, give a first validation of the model extension. Finally, simulations of quasi-static crash box tests are compared to experimental data.

Keywords:

crash analysis, cohesive zone model, structural adhesive bonding, fracture mechanics

1 Experimental Results and Model Extension

The fracture behaviour of the structural adhesive SikaPower498™has been studied experimentally in Tapered Double Cantilever Beam (TDCB) tests for mode I fracture and in End-Loaded Shear Joint (ELSJ) tests for mode II fracture, respectively. Evaluation of those tests give the model parameters GIC and $GIIC$, which are requested by the cohesive zone model MAT_240 in LS-DYNA. In this paper, the dependence of the fracture energies on the thickness of the adhesive layer is studied. Five nominal adhesive layer thicknesses ranging from $0.25\,\mathrm{mm}$ to $4.0\,\mathrm{mm}$ have been investigated. The adherends of all tested specimens consist of steel 1.6358 of $b = 5\,\mathrm{mm}$ thickness. Cohesive fractures occurred in all tests.

1.1 TDCB tests

The fracture behaviour under mode I loading is investigated using two different TDCB specimen types with different dimensions as depicted in Figure 1.
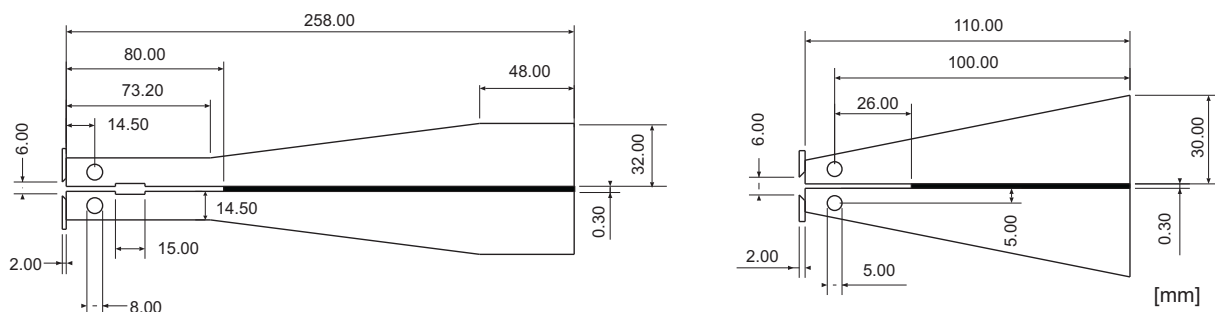

Figure 1: Dimensions of the used TDCB specimen types 1 (left) and 2 (right)

The tests with TDCB specimen type 1 are evaluated using the Irwin-Kies equation (Eq. 1),

$$G_{Ic} = \frac{F^2}{2b}\frac{dC}{da},\tag{1}$$

the tests with the second TDCB specimen type are evaluated by a linear regression between crack growth length and dissipated energy as proposed in [1].

When using specimen type 1 and the Irwin-Kies equation, a plateau force F is averaged during the period of crack propagation. The change of compliance with crack growth $dC/da = 3.56 \times 10^{-5}\,\mathrm{N}^{-1}$ is a constant value for the present geometry. For the evaluation method based on a linear regression line, specimen type 2 is loaded and unloaded in the pin hole, where a certain decrease ΔF of the measured force F triggers the start of unloading. Different crack growth lengths Δa have to be enforced in a test series. The total energy per specimen width W_{tot}/b, which is dissipated by local plastic deformation and fracture of the adhesive layer, is calculated by integration of the measured force displacement curve,

$$W_{tot}/b = \frac{1}{b}\int F\,du,\tag{2}$$

where u denotes the cross head displacement in the line of load introduction. When fitting the crack growth length Δa to the dissipated energy W_{tot}/b by a linear regression, the slope of the regression line is interpreted as the critical energy release rate, G_{Ic}, and the intercept with the energy axis gives the so called crack initiation energy under mode I, $W_{init,I}$. The tests were done at a constant cross head displacement rate, $\dot{u} = 1.7 \times 10^{-2}\,\mathrm{mm/s}$, the unloading rate in the TDCB type 2 $\dot{u} = 8.3 \times 10^{-2}\,\mathrm{mm/s}$ has been chosen.

TDCB specimen type 1   Figure 2 shows the measured force-displacement curves of all experiments. Four specimens were tested in each test series.
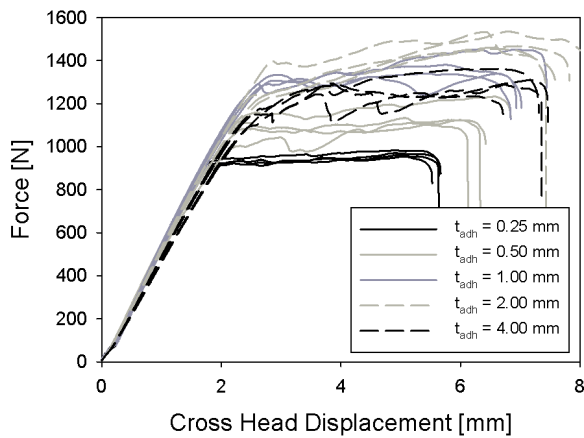
Figure 2: Measured force-displacement curves of TDCB tests - specimen type 1

The critical energy release rate, G_{Ic}, is evaluated by the Irwin-Kies equation (equation 1). The measured force is averaged during the period of crack growth.

TDCB specimen type 2   Alternatively to the usage of the Irwin-Kies equation, G_{Ic} may also be obtained by a correlation between crack growth length and dissipated energy using the smaller type 2 geometry. An amount of 10 to 14 single tests has been done per test series to ensure a proper quality of the found regressions. Figure 3 shows the single test results graphically, with a linear regression line for each test series. G_{Ic} is determined from the slope of the linear regression.
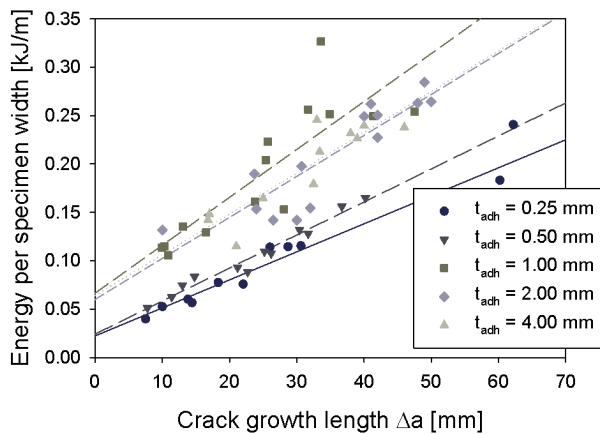

Figure 3: TDCB specimen type 2: W_{tot} vs. Δa

Summary of TDCB test results   The results of the TDCB tests are summarized in figure 4. The results obtained with the both methods agree well for thin adhesive layers. This behaviour was already observed earlier with the crash-optimized adhesive Henkel Terokal 5077™ [1]. Nevertheless, with increasing adhesive thickness, $t_{adh} \geq 1\,\mathrm{mm}$, larger differences between the results achieved with the both methods can be seen. Furthermore, G_{Ic} seems to reach a plateau value for those adhesive layers, which are thicker than $1\,\mathrm{mm}$. The plateau values, which are obtained with the two evaluation methods, differ by a factor of about 1.5, with the smaller value for specimen type 2.

For the extension of the cohesive zone model MAT_240 [2] in LS-DYNA, the dependence of G_{Ic} on the adhesive layer thickness t_{adh} is implemented by a non-linear function of regression,

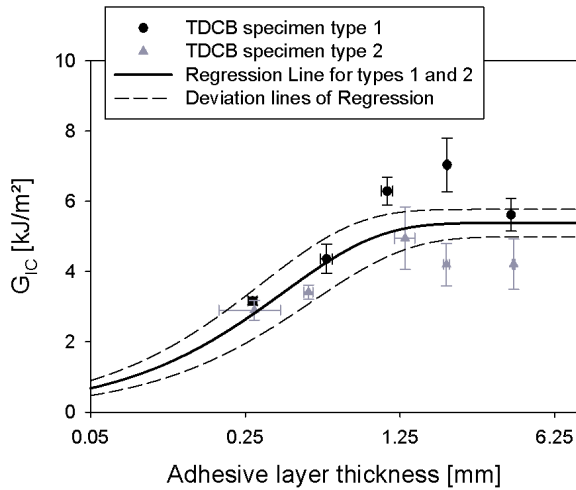$$G_{Ic}\left(t_{adh}\right) = \gamma_I \left(1 - e^{-\tau_I t_{adh}}\right), \tag{3}$$

Figure 4: Critical energy release rate G_{Ic} vs. adhesive layer thickness t_{adh}

with parameters $\gamma_I = 5.38 \pm 0.39\,\mathrm{kJ/m^2}$ and $\tau_I = 2.69 \pm 0.70\,\mathrm{mm^{-1}}$. This function of regression has been fitted to all experimental data, which means that the results of both evaluation methods are included.

1.2 ELSJ tests

The critical energy release rate of adhesive joints under shear loading, G_{IIc}, is commonly evaluated in End-Loaded Split (ELS) tests [3] or in End-Notched Flexure (ENF) tests [4]. Those tests often lead to practical problems when testing structural, crash-optimized adhesives. Even if some recently developed analytical evaluation methods exist, which allow the adherends of the specimens to deform plastically [5], the adherends can not be re-used in that case. The End-Loaded Shear Joint (ELSJ) specimen [6] possesses advantages in case of high-strength adhesives and is used here to determine the dependence of G_{IIc} on the adhesive layer thickness, t_{adh}. Figure 5 shows the dimensions of an ELSJ specimen.
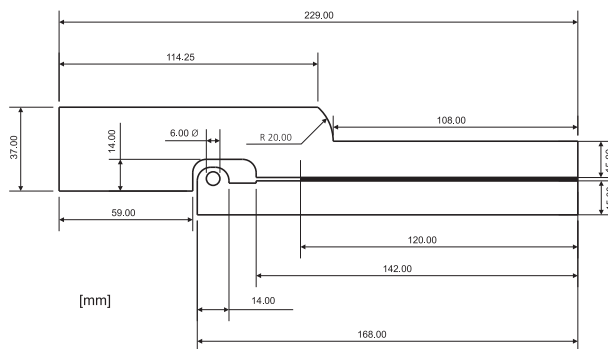

Figure 5: Dimensions of the ELSJ specimen

In an ELSJ test, the adhesive layer is loaded in shear. When a crack propagation is enforced in the adhesive layer, the test is evaluated in the same way as the TDCB tests with specimen type 2. The energy, which is dissipated during the test, is obtained by integration of the force-displacement curve (equation 2) and the corresponding crack growth length is measured on the fracture surface of the specimen after the test. The specimens were loaded with a constant cross head displacement rate, $\dot{u} = 1.7 \times 10^{-2}\,\mathrm{mm/s}$ and an unloading rate $\dot{u} = 1.7 \times 10^{-1}\,\mathrm{mm/s}$, respectively. An amount of 10 to 14 specimens per series has been tested to ensure a proper quality of the found regressions. Figure 6 shows the achieved results for the five investigated nominal adhesive layer thicknesses.
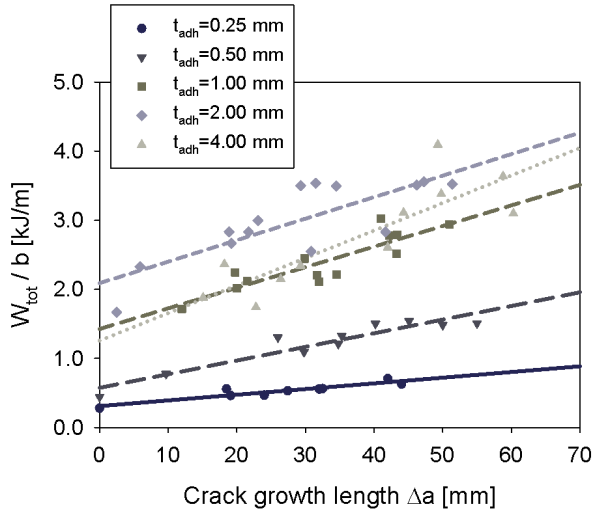

Figure 6: ELSJ tests: W_{tot} vs. Δa

G_{IIc} is obtained from the slope of the linear regression lines plotted in figure 6. The experimentally detected dependence of G_{IIc} on the adhesive layer thickness t_{adh} is approximated for the implementation into LS-DYNA by the same shape of non-linear function of regression, which has been chosen in the case of mode I fracture,

$$G_{IIc}\left(t_{adh}\right) = \gamma_{II}\left(1 - e^{-\tau_{II}t_{adh}}\right), \tag{4}$$

with parameters $\gamma_{II} = 38.03 \pm 2.84\,\text{kJ/m}^2$ and $\tau_{II} = 1.26 \pm 0.27\,\text{mm}^{-1}$. Figure 7 shows the experimental data and the regression line for the dependence of G_{IIc} on t_{adh}.
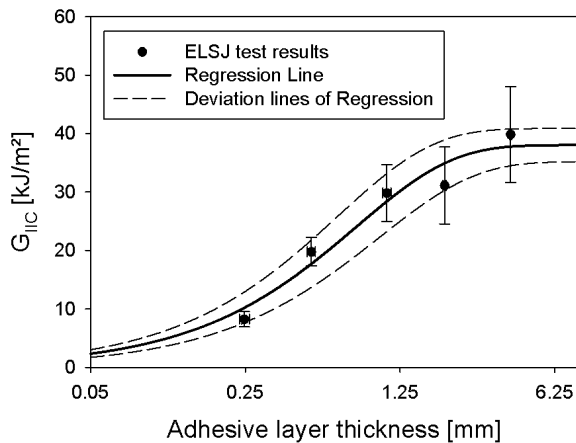

Figure 7: Critical energy release rate G_{IIc} vs. adhesive layer thickness t_{adh}

1.3 Model Extension

MAT_240 is a rate-dependent, elastic-plastic cohesive zone model, which is available in LS-DYNA™ from release LS971 R5 or higher. A detailed documentation of the model can be found in [2]. Here, this model has been extended via an user-defined subroutine to a dependence of the both model parameters GIC and $GIIC$ on the adhesive layer thickness as experimentally detected. The dependence of the critical energy release rate under mode I loading, G_{Ic}, is given by equation 3, while the corresponding relation of G_{IIc} is described by equation 4, respectively.

The thickness-dependence of the yield stress parameters T and S has not been investigated here. Therefore, no such dependence has been considered in the model extension. Furthermore no rate-dependency of any of the cohesive zone model parameters has been taken into account, since the previously described experimental tests have been carried out at quasi-static conditions only.

First validations and a first application of the extended model are shown in the next chapter.

2 Application of Extended Model

The extended MAT_240 is used in simulations of asymmetric tapered double cantilever beam (ATDCB) tests. The ATDCB test is a fracture mechanical test under mixed-mode loading as proposed by Park and Dillard [7]. Furthermore, the extended model has been applied in the simulation of crash-box tests at quasi-static load conditions. Cohesive fracture of the adhesive layer occured in all tests.

2.1 Simulation of ATDCB tests

ATDCB specimens were fabricated from adherends of steel of $t = 5\,\mathrm{mm}$ width. The crash-optimized adhesive SikaPower498™ has been used to join the adherends as in the TDCB and ELSJ tests described in the previous section. Figure 8 shows the dimensions of an ATDCB specimen, which is loaded in its pin-holes.
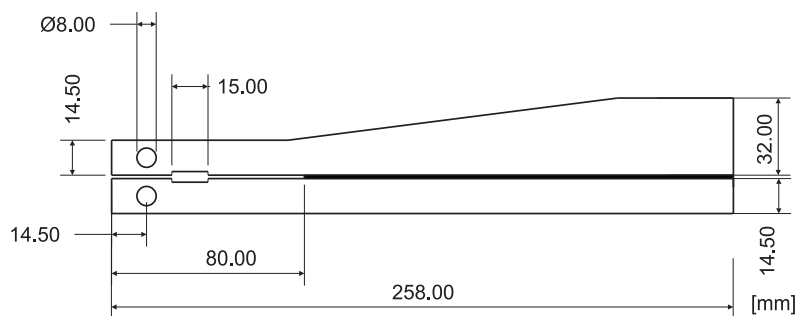

Figure 8: Dimensions of an ATDCB specimen

In the finite element model of the ATDCB tests, reduced integrated solid elements have been chosen to model the adherends, while the adhesive layer has been modelled with cohesive elements (Solid type 19) and the extended MAT_240, which considers the dependence of the fracture energies on the adhesive layer thickness. Constant values for the elastic moduli and the yield stress parameters have been chosen, the fracture energies were modelled as dependent on the adhesive layer thickness as discussed before.

Specimens with five nominal adhesive layer thicknesses have been tested. The experimentally measured force-displacement curves are compared to numerical predictions in the figures 9 to 13. In the experiments, the initial distance from the line of load introdution to the current crack tip was larger than in the corresponding numerical models, therefore the specimens behave stiffer in all simulations than observed in the tests. Further simulations have been done with parameters describing the upper and the lower confidence interval of the fuctions of regressions as shown in the figures 4 and 7.
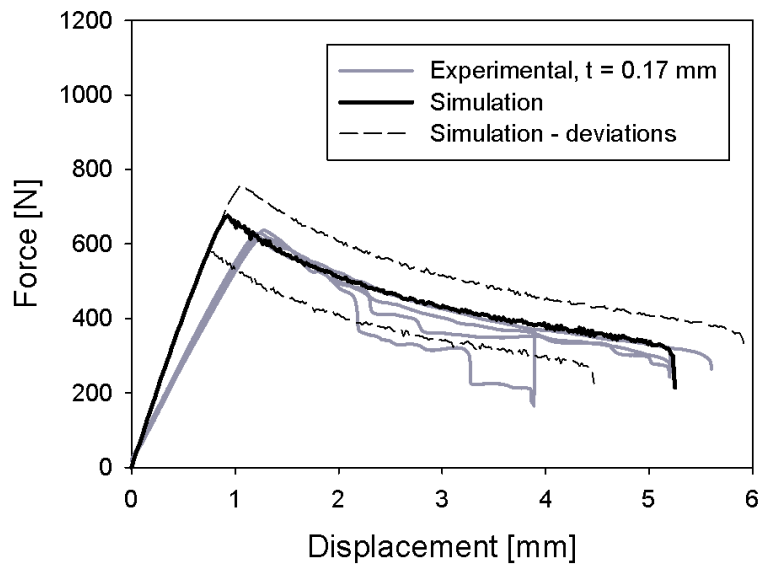
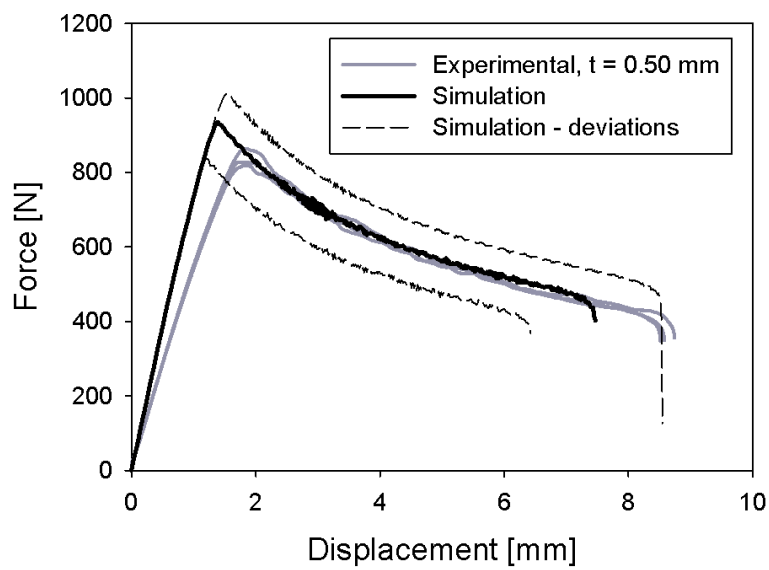*Figure 9:* ATDCB tests: comparison between experimental and numerical data, $t_{adh} = 0.17\,\mathrm{mm}$

Figure 10: ATDCB tests: comparison between experimental and numerical data, $t_{adh} = 0.5\,\mathrm{mm}$
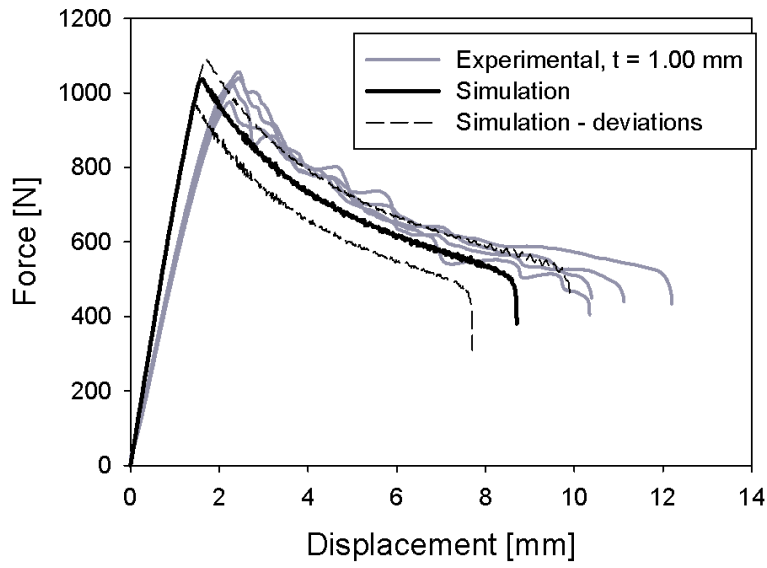
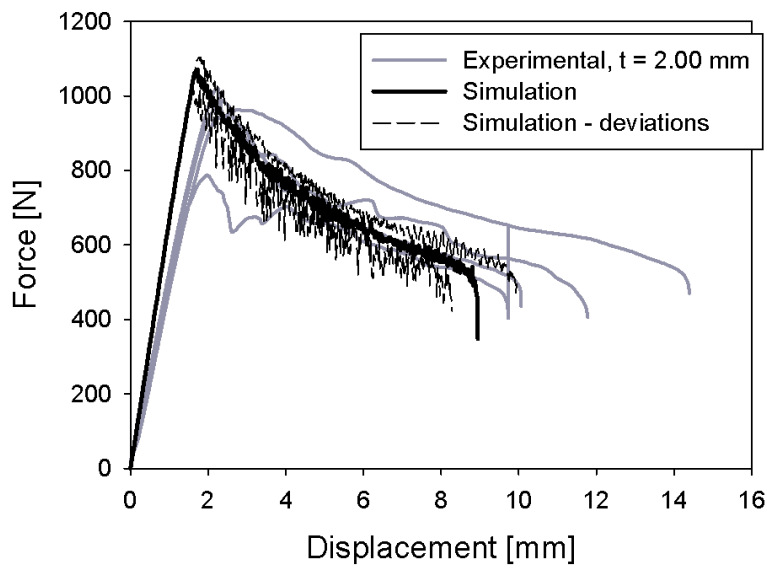*Figure 11:* ATDCB tests: comparison between experimental and numerical data, $t_{adh} = 1.0\,\text{mm}$

Figure 12: ATDCB tests: comparison between experimental and numerical data, $t_{adh} = 2.0\,\text{mm}$
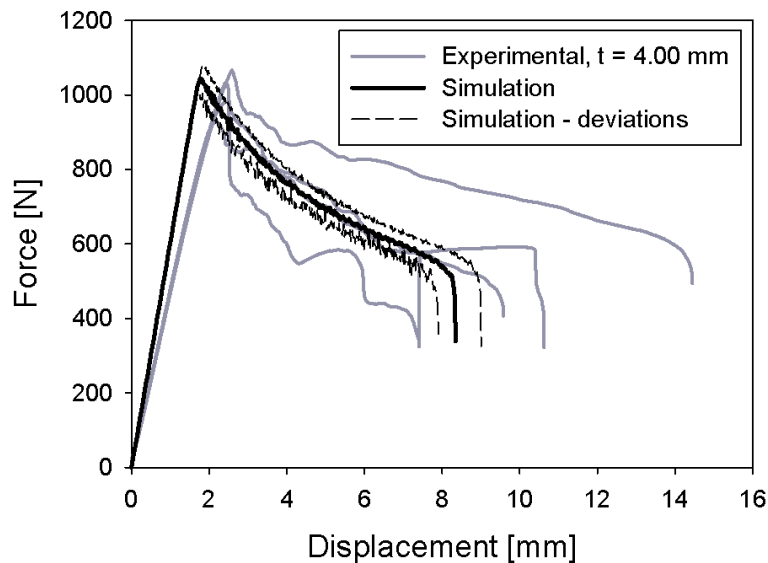
Figure 13: ATDCB tests: comparison between experimental and numerical data, $t_{adh} = 4.0\,\mathrm{mm}$

Despite of the differences in the initial stiffness, a good correlation between experimental and numerical data could be achieved by the simulations. Since the force-displacement curves obtained in an ATDCB test depend strongly on both fracture energies, G_{Ic} and G_{IIc}, the agreement between numerical and experimental data can be interpreted as first successfull validation of the model extension with respect to the influence of the adhesive layer thickness on the fracture behaviour of the bonded joints.

2.2 Simulation of Crash Box Tests

Crash boxes have been manufactured from automotive steel and the structural adhesive SikaPower498™. The flanges of two cap profiles are joined by an adhesive bond of varying thickness between zero and $3\,\mathrm{mm}$. Figure 14 gives a detailed top view on a bonded flange. Two crash box samples have been tested under compression at quasi-static load conditions.
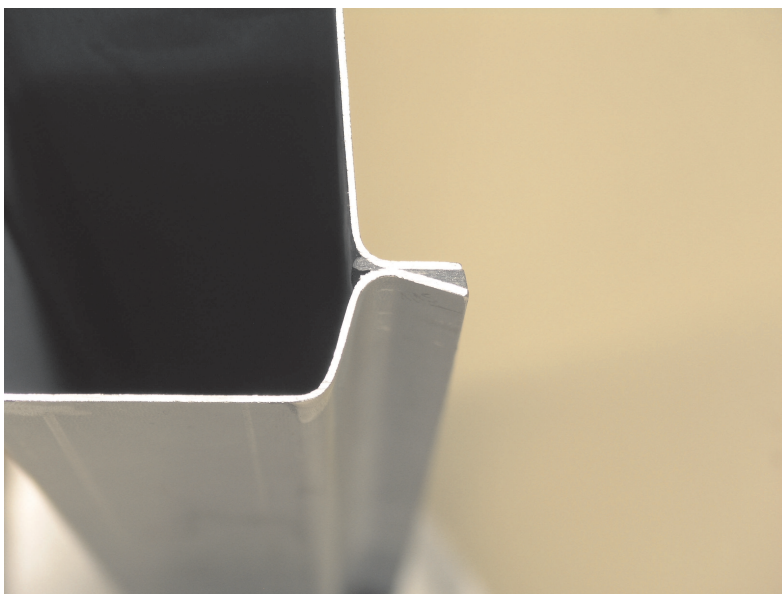

Figure 14: Crash box: Detail of bondend flange connection with adhesive layer of varying thickness

In the corresponding finite element model, the profiles have been modelled with reduced-integrated shell elements, while cohesive elements (solid type 19) with the extended MAT_240 have been chosen for the adhesive layer. The boundary conditions of the crash box tests have been chosen in the simulations as in the tests.
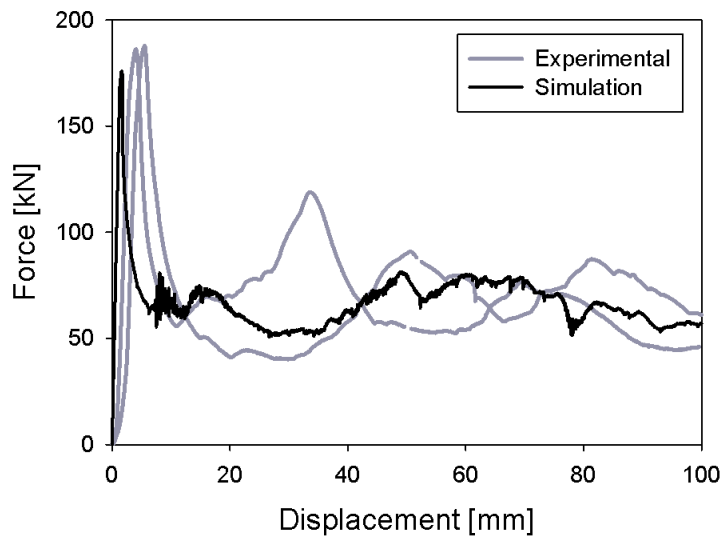

Figure 15: Crash box tests: Experimental and numerical force-displacement-curves

Figure 15 depicts the force-displacment-curves recorded during the tests with a numerical prediction. A good agreement between both is observed, for the initial peak force as well as for the following plateau region.

Figure 16: Crash box tests: Comparison of deformed shapes (left: experimental, right: simulation)

Figure 16 compares the deformations and the failure of the adhesive layer, observed in the experimental tests and the simulations. A good agreement is achieved here as well.

3 Conclusions

This work presents an extension of the cohesive zone model MAT_240. When modelling an adhesive layer with that material model, the fracture energies in both mode I and mode II become dependent on the thickness of the adhesive layer. The regressions between fracture energy and adhesive layer

thickness, which are considered by the model extension, have been detected in fracture mechanical tests with the adhesive SikaPower498™.

A first validation of the model extension is given by the comparison of experimental results of asymmetric tapered double cantilever beam (ATDCB) tests with different adhesive layer thicknesses to numerical results. Furthermore, the extended model has been used in the simulation of a crash box test, where the crash boxes have been manufactured with adhesive layers of varying thickness. A good agreement between the experimental results and the numerical predictions is observed in that case as well.

The presented model extension does neither include rate-dependent effects nor a dependence of the yield stresses on the adhesive layer thickness. However, the usage of the extended model leads to satisfying results at quasi-static load conditions. Its applicability in dynamic crash simulations has still to be investigated.

4 Literature

[1] S. Marzi, O. Hesebeck, M. Brede, and F. Kleiner. A rate-dependent cohesive zone model for adhesive layers loaded in mode I. *J. Adh. Sc. Tech.*, 23:881–898, 2009.

[2] S. Marzi, O. Hesebeck, M. Brede, and F. Kleiner. A rate-dependent, elasto-plastic cohesive zone mixed-mode model for crash analysis of adhesively bonded joints. In *7th European LS-DYNA conference*, 2009.

[3] B.R.K. Blackman, A.J. Kinloch, and M. Paraschi. The determination of the mode ii adhesive fracture resistance, giic, of structural adhesive joints: an effective crack length approach. *Engrg. Frac. Mech.*, 72:877–897, 2005.

[4] K. Leffler, K.S. Alfredsson, and U. Stigh. Shear behaviour of adhesive layers. *Int. J. Solids and Structures*, 44:530–545, 2006.

[5] U. Stigh, K.S. Alfredsson, and A. Biel. Measurement of cohesive laws and related problems. In *Proceedings of the ASME International Mechanical Engineering Congress and Exposition*, November 13-19 2009.

[6] S. Marzi, O. Hesebeck, M. Brede, and F. Kleiner. An end-loaded shear joint (ELSJ) specimen to measure the critical energy release rate in mode II of tough, structural adhesive joints. *J. Adh. Sc. Tech.*, 23:1883–1891, 2009.

[7] S. Park and D.A. Dillard. Development of a simple mixed-mode fracture test and the resulting fracture energy envelope for an adhesive bond. *Int. J. Fract.*, 148:261–271, 2007.